The RSPO–LGR4/5–ZNRF3/RNF43 module controls liver zonation and size

Citation for published version:
Plana-Paz, L, Orsini, V, Boulter, L, Calabrese, D, Pikiolek, M, Nigsch, F, Xie, Y, Roma, G, Donovan, A, Marti, P, Beckmann, N, Dill, MT, Carbone, W, Bergling, S, Isken, A, Mueller, M, Kinzel, B, Yang, Y, Mao, X, Nicholson, TB, Zamponi, R, Capodieci, P, Valdez, R, Rivera, D, Loew, A, Ukomadu, C, Terracciano, LM, Bouwmeester, T, Cong, F, Heim, MH, Forbes, SJ, Ruffner, H & Tchorz, JS 2016, 'The RSPO–LGR4/5–ZNRF3/RNF43 module controls liver zonation and size', *Nature Cell Biology*, vol. 18, no. 5, pp. 467–479. https://doi.org/10.1038/ncb3337

Digital Object Identifier (DOI):
10.1038/ncb3337

Link:
Link to publication record in Edinburgh Research Explorer

Document Version:
Peer reviewed version

Published In:
Nature Cell Biology

The RSPO-LGR4/5-ZNRF3/RNF43 module controls liver zonation and size

Planas-Paz L[1,*], Orsini V[1,*], Boulter L[2], Calabrese D[3], Pikiolek M[1], Nigsch F[1], Xie Y[4], Roma G[1], Donovan A[4], Marti P[1], Beckmann N[1], Dill MT[3], Carbone W[1], Bergling S[1], Isken A[1], Mueller M[1], Kinzel B[1], Yang Y[4], Mao X[4], Nicholson TB[4], Zamponi R[4], Capodieci P[4], Valdez R[4], Rivera D[4], Loew A[4], Ukomadu C[4], Terracciano LM[5], Bouwmeester T[1], Cong F[4], Heim MH[3], Forbes SJ[6], Ruffner H[1], Tchorz JS[1#]

[1]Novartis Institutes for BioMedical Research, Novartis Pharma AG, Basel, Switzerland

[2]MRC Human Genetics Unit, Institute of Genetics and Molecular Medicine, University of Edinburgh, Edinburgh, UK

[3]Division of Gastroenterology and Hepatology, University Hospital Basel, Basel, Switzerland

[4]Novartis Institutes for BioMedical Research, Novartis Pharma AG, Cambridge, MA

[5]Institute for Pathology, University Hospital Basel, Basel, Switzerland

[6]MRC Centre for Regenerative Medicine, University of Edinburgh, Edinburgh, UK

[*]These authors contributed equally

#Correspondence should be addressed to: Jan Tchorz, Novartis Campus, 4002 Basel, Switzerland, phone: +41798634285, Email: jan.tchorz@novartis.com

Key words: Wnt, lineage tracing, liver regeneration, liver development

LGR4/5 receptors and their cognate RSPO ligands potentiate Wnt/β-Catenin signalling and promote proliferation and tissue homeostasis in epithelial stem cell compartments. In the liver, metabolic zonation requires a Wnt/β-Catenin signalling gradient, but the instructive mechanism controlling its spatiotemporal regulation is not known. We have identified a novel role for the RSPO-LGR4/5-ZNRF3/RNF43 module as master regulator of Wnt/β-Catenin-mediated metabolic liver zonation. Liver-specific LGR4/5 loss-of-function (LOF) or RSPO blockade disrupted hepatic Wnt/β-Catenin signalling and zonation. Conversely, pathway activation in ZNRF3/RNF43 LOF mice or with recombinant RSPO1 protein expanded the hepatic Wnt/β-Catenin signalling gradient in a reversible and LGR4/5-dependent manner. Furthermore, we show that LGR4+ hepatocytes throughout the lobule contribute to liver homeostasis and regeneration. Likewise, recombinant RSPO1 protein increased liver size and improved liver regeneration, whereas LGR4/5 LOF caused the opposite effects, resulting in hypoplastic livers. Together, the RSPO-LGR4/5-ZNRF3/RNF43 module controls metabolic liver zonation and acts as a hepatic growth/size rheostat during development, homeostasis and regeneration.

Hepatic zonation and organ size control are required for physiological liver function, including metabolization of a wide range of endogenous products and xenobiotics. Hepatocyte function is determined by its position along the porto-central axis of the liver lobule, which creates a metabolic zonation in the liver. Complementary metabolic pathways occur within non-overlapping liver zones, thus maintaining optimal metabolic homeostasis [1-5]. Physiological liver size is tightly controlled by the concerted growth of hepatocytes and other hepatic cells during development, homeostasis and regeneration [6-8]. Recent studies have highlighted the Wnt/β-Catenin pathway as a major regulator of liver zonation, development and regeneration [4, 9-11]. Wnt pathway activation stimulates cytoplasmic stabilization and nuclear translocation of β-Catenin, which subsequently associates with transcriptional regulators to control β-Catenin target gene expression (*e.g.* Axin2 and leukocyte cell-derived chemotaxin 2 (Lect2)) and expression of other Wnt/β-Catenin-dependent genes (*e.g.* Glutamine synthetase (GS) and Cyp2e1) [12]. β-Catenin-deficient mouse livers exhibit defects in metabolic liver zonation [10]. The Adenomatous polyposis coli (APC) protein antagonizes β-Catenin activity, since APC deletion activates β-Catenin signalling and thereby expands the hepatic Wnt activity gradient [9, 13]. Deletion of β-Catenin impaired hepatocyte proliferation during liver development and regeneration, whereas transgenic β-Catenin overexpression or APC deletion results in hyperplastic livers and hepatocellular carcinoma due to increased hepatocyte proliferation [14-19]. However, the instructive molecular cues for spatiotemporal control of Wnt/β-Catenin signalling in liver zonation, development and regeneration have remained elusive.

R-Spondin (RSPO)1-4 ligands potentiate Wnt/β-Catenin signalling via Leucine-rich repeat containing G protein-coupled receptors 4-6 (LGR4-6) [20-23]. In the absence of RSPO proteins, Wnt signal transduction is negatively regulated by cell-surface transmembrane E3 ubiquitin ligases, Zinc and ring finger 3 (ZNRF3) and its homologue Ring finger 43 (RNF43), which both promote Wnt receptor turnover. Upon stimulation, RSPO proteins bind to LGR4/5 receptors as well as the ZNRF3/RNF43 transmembrane ubiquitin ligases, causing the latter to become cleared from the plasma membrane which leads to increased Wnt signalling [24, 25]. We and others have shown that RSPO-LGR4/5-ZNRF3/RNF43 signalling plays an essential role in developing and maintaining various epithelial tissue stem cell compartments by regulating tissue homeostasis [21, 23, 26, 27]. The liver has a remarkable plasticity with an intrinsically high capacity for context-dependent regeneration in response to diverse injuries and during homeostasis [28-32]. LGR5 has been reported to be exclusively expressed around the portal vein only following injury [33, 34], whereas undamaged livers have persistent high Wnt/β-Catenin activity around the central vein [1, 35]. This is in contrast to other tissues where cells with high Wnt/β-Catenin activity express LGR4 and LGR5 to mediate RSPO-mediated Wnt/β-Catenin signalling [21, 23, 26, 27]. A potential role of RSPO-LGR4/5-ZNRF3/RNF43 signalling in the regulation of hepatic Wnt/β-Catenin activity during liver development, homeostasis and regrowth has remained unclear.

Through integrated *in vivo* approaches comprising lineage tracing, tissue-specific LGR4/5 LOF, pathway activation via RSPO1 injections or ZNRF3/RNF43 LOF and RNA expression analyses we have identified a novel role for the RSPO-LGR4/5-ZNRF3/RNF43 module in controlling metabolic liver zonation. We further show that the RSPO-LGR4/5-ZNRF3/RNF43 module acts as a hepatic growth/size rheostat during development, homeostasis and regeneration and that recombinant RSPO1 protein administration accelerates liver regrowth.

LGR4 and LGR5 are co-expressed in pericentral hepatocytes with high Wnt activity

To gain a detailed resolution of the hepatic Wnt/β-Catenin signalling gradient regulating metabolic liver zonation, we assessed Wnt/β-Catenin activity in different hepatic zones using immunostaining, *in situ* hybridization (ISH) and transgenic reporter mice. Expression of GS, a Wnt/β-Catenin-dependent gene and key enzyme in the ammonia detoxification pathway [10] (Figure 1a, 1c) as well as β-Catenin reporter activity in Tcf/Lef-Venus mice [36] (Figure 1b, 1c), were restricted to the first layers of hepatocytes around the central vein. Similarly, ISH showed that Axin2 mRNA was predominantly expressed in these cells (Figure 1d, 1e). Expression of CYP2E1, another metabolic enzyme and Wnt/β-Catenin-dependent gene [37], extended into the parenchyma adjacent to the central veins (Figure 1a, 1c). This suggests differential expression of Wnt/β-Catenin-dependent genes along the centro-portal Wnt/β-Catenin signalling gradient possibly because of different inductive thresholds or transcriptional regulation for these genes. To explore whether the RSPO receptors LGR4 and LGR5 and the ubiquitin ligases ZNRF3 and RNF43 contribute to the regulatory network that establishes the Wnt/β-Catenin signalling gradient and liver zonation, we performed a detailed expression analysis. Using ISH staining in wild type mice, we found Lgr5 expression mainly restricted to pericentral hepatocytes with high Wnt activity. Almost all hepatocytes adjacent to the central vein, mono- and bi-nucleated, expressed Lgr5. The number of Lgr5-positive hepatocytes slightly decreased in the 2nd and 3rd pericentral layers, whereas only a negligible minority of parenchymal hepatocytes expressed Lgr5. Lgr4, which was coexpressed with Lgr5 in pericentral hepatocytes, was expressed in virtually all hepatocytes across the liver lobule (Figure 1f, 1g; Supplementary Figure 1a, 1b). Znrf3 was broadly expressed in hepatocytes throughout liver (Figure 1h, 1i), whereas mice that express LacZ from the *Rnf43* locus (Supplementary Figure 2a) showed that Rnf43 expression was restricted to central vein hepatocytes (Figure 1j, 1k), similar as seen for Lgr4 and Lgr5, respectively. To further explore the expression profiles and roles of Lgr4 and Lgr5 in the liver, we performed lineage tracing experiments using mice expressing tamoxifen (TAM)-inducible Cre (CreERT2) from the Lgr4 (Lgr4ki mice) or Lgr5 (Lgr5ki mice) loci [26], crossed with Rosa26 (R26)-β-Galactosidase (β-Gal; LacZ) [38], R26-tdTomato (tdTOM) or R26-enhanced green fluorescent protein (EGFP) reporter mice (Supplementary Figure 3a). Ten-day lineage tracing in Lgr4ki/R26-LacZ mice labelled hepatocytes throughout the liver, confirming broad LGR4 expression (Figure 2a, Supplementary Figure 3b). Ten-month LGR4 lineage tracing in these mice showed a similar expression pattern with small LacZ+ hepatocyte clones consisting of 1-5 cells, in line with low rates of homeostatic cell division [5] (Figure 2b, 2c, Supplementary Figure 3b). Similarly sized clones of LGR4 lineage-traced pericentral, parenchymal and periportal hepatocytes are indicative of similar proliferation rates within the 3 different liver zones (Figure 2c). Ten-day lineage tracing in Lgr5ki/R26-LacZ mice confirmed that LGR5 expression is restricted to pericentral hepatocytes (Figure 2d, Supplementary Figure 3c). Eighteen-month lineage tracing and distributions analysis across different zones indicated that LGR5+ hepatocytes remained at the central vein as small clones consisting of 1-5 cells and do not radiate out into the parenchyma (Figure 2e, 2f, Supplementary Figure 3c, 3d). Co-expression of Axin2 and Lgr5 in virtually all of the

LGR5 lineage-traced hepatocytes, as measured by ISH, confirmed active Wnt signalling in these cells similar as in untraced neighbouring pericentral hepatocytes (Supplementary Figure 3e-g). Moreover, Ki67 staining in the LGR5 lineage-traced hepatocytes 48 h post-partial hepatectomy (PH) indicated that the proliferation capacity of these cells was similar compared to untraced neighbouring pericentral hepatocytes (Supplementary Figure 3h-j). A comparative 7-day EdU proliferation analysis in Lgr5ki and wt mice showed that the absence of one of the Lgr5 alleles did not impair homeostatic proliferation of pericentral hepatocytes (Figure 2i, 2j). Ten-day lineage tracing in Lgr4ki/R26-EGFP mice (Figure 2g) and Lgr5ki/R26-tdTOM mice (Figure 2h) and co-staining of labelled cells with hepatocyte markers Hepatocyte Nuclear Factor 4 Alpha (HNF4α) or GS, respectively, confirmed that the traced cells were indeed hepatocytes. In gut and skin, LGR4 is more broadly expressed than LGR5, and LGR5 expression is restricted to tissue stem cells with high Wnt activity. Concurrently, LGR5 is a Wnt target gene itself [39-41]. Similarly, we observed a broad expression of LGR4 in hepatocytes throughout the liver, while LGR5 expression was restricted to pericentral hepatocytes with high Wnt activity. Despite persistent high Wnt activity and LGR5 expression, pericentral hepatocytes rarely proliferated and did not exhibit increased proliferation rates when compared to those of other hepatic zones, as indicated both by EdU labelling (Figure 2i, 2k-m and Supplementary Figure 3k-n) and Ki67 staining (Figure 2n-p). This is in contrast to actively cycling LGR5+ cells in tissue stem cell compartments of other organs [27], but consistent with similar homeostatic proliferation rates across different liver zones reported earlier [42]. In undamaged livers, the majority (>80%) of proliferating cells were found in the liver parenchyma (Figure 2m, 2p, and Supplementary Figure 3n), itself the largest hepatic zone, indicating that parenchymal hepatocytes account for the majority of new hepatocytes during liver homeostasis. This is consistent with previous reports showing that the majority of proliferating hepatocytes reside in the parenchyma and that hepatocytes throughout the lobule contribute to liver homeostasis without zonal dominance [42-44].

LGR4 and LGR5 receptors are essential for metabolic liver zonation

To delineate whether LGR4 and LGR5 are mediating the instructive cues that establish the hepatic Wnt/β-Catenin signalling gradient and liver zonation, we generated liver-specific Lgr4 knock-out (KO) (Lgr4LKO), Lgr5KO (Lgr5LKO) and Lgr4/5 double KO (Lgr4/5dLKO) mice using Albumin (Alb)Cre-mediated deletion (Supplementary Figure 2b). Mice of all 3 genotypes were born at normal Mendelian ratios and viable with normal lifespans (data not shown). Lgr4LKO and Lgr4/5dLKO, but not Lgr5LKO mice showed reduced liver weight when compared to control mice (Figure 3a). Loss of Lgr4 and Lgr5 mRNA in the liver was confirmed by reverse transcription polymerase chain reaction (RT-PCR) (Figure 3b) and ISH (Figure 3c). While no overt changes were observed in Lgr5LKO mice, Wnt signalling was abrogated in Lgr4/5dLKO and Lgr4LKO mice, as indicated by loss of Axin2 and Lect2 expression. Lgr5 mRNA expression was absent in Lgr4LKO mice (Figure 3b, 3c), similar as we previously reported for the developing intestinal epithelium [26]. This suggests a dominant role for LGR4 over LGR5, and that loss of Lgr5 expression is a result of abrogated Wnt signalling. GS staining was severely reduced in Lgr4LKO and completely lost in Lgr4/5dLKO mice, whereas Lgr5LKO mice had slightly elevated GS expression when compared to control mice (Figure 3d, 3e). Likewise, LGR4 and LGR4/5 deletion resulted in impaired CYP2E1 expression (Figure 3f, 3g). Early postnatal analysis of Lgr4/5dLKO mice showed reduced GS expression already at postnatal day (P)2 which remained low on P10 and P30, whereas it was increased in control mice from P2 to P10 (Supplementary Figure 4a, 4b). P2, P10 and P30 Lgr4/5dLKO mice showed functional hepatocyte and biliary cell differentiation during liver development, as evidenced by normal distribution of HNF4α+ hepatocytes, SRY (Sex Determining Region Y)-Box 9 (SOX9)+/Cytokeratin 19 (CK19)+ biliary ducts and absence of SOX9 in hepatocytes (Supplementary Figure 4c, 4d), excluding the possibility that compromised hepatocyte differentiation during liver development accounts for the impaired metabolic zonation. To gain further insights into the mechanistic consequences of liver-specific LGR4/5 deletion, we performed high-throughput RNA sequencing (RNA-Seq) on total liver RNA samples isolated from control and Lgr4/5dLKO mice. Expression of Wnt target genes (*e.g.* Axin2, Lect2 and Tumor Necrosis Factor Receptor Superfamily, Member 19 (Tnfrsf19; Troy)) as well as gene sets for Wnt signalling and metabolic processes were significantly downregulated in livers with combined LGR4 and LGR5 deletions (Supplementary Figure 5a, 5b, Supplementary Table 1, 2). Comparative expression analysis of genes encoding for metabolic enzymes [45] revealed that pericentrally expressed metabolic genes were downregulated, whereas few periportal genes (Hsd17b13 and Hal) were upregulated in Lgr4/5dLKO compared to control mice (Figure 3h, Supplementary Figure 5a). RT-PCR analysis confirmed downregulation of pericentral metabolic genes (Glul, Cyp2e1 and Cyp1a2) and upregulation of Hsd17b13 and Hal (Figure 3i, 3j). This indicates that loss of hepatic Wnt/β-Catenin signalling in Lgr4/5dLKO mice results in loss of metabolic liver zonation. RT-PCR and immunostaining confirmed that periportal metabolic genes, that were upregulated in β-Catenin KO mice or mice with virus-mediated DKK1 overexpression [9, 13], were not upregulated in Lgr4/5dLKO compared control mice (Figure 3j; Supplementary Figure 5c, 5d). It is possible that inactivation or deletion of Wnt pathway components at different hierarchical levels result in distinct signalling output events which might account for these differences; *e.g.* LGR4/5 deletion was also shown to impair non-canonical Wnt signalling, in contrast to β-Catenin deletion or DKK1 overexpression [22, 46]. Moreover, downregulated gene sets involved in cell cycle regulation further suggest a role for LGR4 and LGR5 in controlling hepatic cell proliferation (Supplementary Figure 5b). Together, we identified an essential role for LGR4 and LGR5 receptors in spatial regulation of the centro-portal Wnt/β-Catenin signalling gradient and metabolic liver zonation.

RSPO controls liver zonation via LGR4 and LGR5 receptors

Overexpression of the extracellular domain (ECD) of ZNRF3 (ZNRF3ECD) was shown to block endogenous RSPO function by blocking RSPO1-induced membrane accumulation of Frizzled proteins [24]. To analyse whether RSPO proteins control the hepatic Wnt/β-Catenin signalling gradient, we generated BAC-transgenic mice that allow doxycycline (DOX)-induced ubiquitous expression of the ZNRF3ECD (Znrf3ECD mice) and crossed these mice with Axin2-LacZ mice to obtain double transgenic Znrf3ECD/Axin2-LacZ mice (Figure 4a). Znrf3ECD/Axin2-LacZ mice fed with DOX-containing diet showed reduced LacZ expression when compared to those with normal diet, indicating that loss of endogenous RSPO function impaired the hepatic Wnt/β-Catenin activity gradient (Figure 4b, 4c). Likewise, GS (Figure 4d, 4e) and CYP2E1 (Figure 4f, 4g) expression was dramatically reduced in Znrf3ECD/Axin2-LacZ mice fed with DOX-containing diet. We next generated mice that allowed for the inducible combined deletion of ZNRF3 and RNF43 using TAM (Znrf3/Rnf43dfl;R26CreERT2 mice) (Figure 4h). TAM injections resulted in a dramatic increase in GS (Figure 4i, 4j) and CYP2E1 (Figure 4k, 4l) expression in Znrf3/Rnf43dfl;R26CreERT2 mice when compared to Znrf3/Rnf43dfl;R26CreERT2 mice without TAM, with CYP2E1 expression even expanding into portal vein hepatocytes (Figure 4k). This indicates that the LGR4/5-ZNRF3/RNF43 complex is a key regulator of the hepatic Wnt/β-Catenin signalling gradient and metabolic liver zonation.

To further study the effect of RSPO in liver zonation, we administered recombinant RSPO1 (10 mg/kg) or PBS twice weekly to Lgr4/5dLKO and control mice for 1 week, 2 weeks and 2 weeks followed by 4 weeks off-treatment (wash-out) (Figure 5a). 2 weeks RSPO1 injection in adult wild type mice and 2 weeks RSPO1 injection in TCF/LEF-Venus mice markedly increased Axin2 mRNA (Figure 5b, 5c) and Wnt/β-Catenin reporter expression (Figure 5d, 5e), respectively. Importantly, RSPO1 injections expanded Wnt/β-Catenin signalling into periportal hepatocytes, indicating that all cells across the liver lobule are competent to respond to Wnt pathway activation and that Wnt receptors and ligands must be available throughout the liver. Likewise, RSPO injections increased GS protein (Figure 5f, 5g) and CYP2E1 protein (Figure 5h, 5i) expression in control mice but not in Lgr4/5dLKO mice when compared to PBS injected mice after 1 week. After 2 weeks, additional RSPO1 injections further expanded GS and CYP2E1 expression, which were reduced to PBS control levels after additional 4 weeks off-treatment (Figure 5f-i). This further indicates that RSPO1 controls hepatic Wnt/β-Catenin signalling in an LGR4/5-dependent manner to confer spatiotemporal regulation of the centro-portal Wnt/β-Catenin activity gradient and metabolic liver zonation. It also indicates that sustained signalling through the RSPO-LGR4/5-ZNRF3/RNF43 module is essential to maintain this zonation. Notably, RSPO1 injections or ZNRF3/RNF43 deletions did not result in immediate ectopic GS expression throughout the liver but caused progressing expansion along the centro-portal axis, similarly to what was observed in *Apc* mutant mice [13]. This suggests the possibility that other mechanisms contribute to regulating zonated GS expression; *e.g.* YAP activity in periportal hepatocytes may restrict GS expression, as it was recently shown that YAP is expressed in a porto-central gradient and can negatively regulate GS [47, 48]. In summary, our data suggest that Wnt receptors and ligands are distributed throughout the liver lobule and that the RSPO-LGR4/5-ZNRF3/RNF43 module is essential for hepatic Wnt signalling and metabolic liver zonation.

<u>LGR4 and LGR5 deletions impair postnatal liver development</u>

Reduced liver weight and downregulation of gene sets involved in cell cycle regulation indicated impaired growth control in Lgr4/5dLKO mice. Analysis of early postnatal development revealed impaired hepatocyte proliferation in Lgr4/5dLKO mice at P2 and P10, whereas no significant difference was observed at P30 with overall reduced proliferation rates (Supplementary Figure 6a-c), as well as in adult mice (data not shown) when compared to control littermates. Notably, impaired proliferation was most evident in pericentral hepatocytes with high Wnt activity. Consequently, liver weight was significantly reduced in P10 and P30 Lgr4/5dLKO mice when compared to control mice, while it was comparable at P2 among both genotypes (Supplementary Figure 6d). To study whether LGR4 and LGR5 are important for controlling proliferation during embryonic liver development we stained E16.5 embryos with full-KO for LGR4, LGR5 and LGR4/5 as well as wild type littermates [26] for Ki67. We did not observe any differences in the proliferative capacity of the liver between the different genotypes (Supplementary Figure 6e, 6f), indicating that LGR4 and LGR5 are dispensable for embryonic liver growth at E16.5. This suggests that reduced liver weight in Lgr4/5dLKO mice is a consequence of impaired hepatocyte proliferation during later stages of liver development.

RSPO controls liver size and regeneration via LGR4/5 receptors

Impaired liver development and liver size in Lgr4/5dLKO mice suggested that RSPO-LGR4/5 signalling might act as a hepatic growth/size rheostat. To further investigate this mechanism, we subjected Lgr4LKO, Lgr5LKO, Lgr4/5dLKO and control mice to PH (Figure 6a). 2 days post-PH, liver weight was significantly reduced in Lgr4LKO and Lgr4/5dLKO but not in Lgr5LKO mice when compared to controls (Figure 6b). Detailed proliferation analysis by Ki67 immunostaining revealed that Lgr4LKO, Lgr5LKO and Lgr4/5dLKO mice showed impaired proliferation in pericentral hepatocytes (Figure 6c). In contrast, proliferation of parenchymal (Figure 6d) and periportal (Figure 6e) hepatocytes was only impaired in Lgr4LKO and Lgr4/5dLKO but not in Lgr5LKO mice when compared to control mice. Zonal differences in proliferation indicate that LGR receptors are required for proliferation in their respective expression zones. Interestingly, during the peak regenerative response post-PH in control mice, hepatocyte proliferation rates were generally lower around the central vein when compared to portal vein and parenchyma (Figure 6c-e). RT-PCR for Axin2 showed activation of the Wnt pathway during liver regeneration (d2 post-PH) in control mice and confirmed lack of Axin2 expression in Lgr4/5dLKO mice (Figure 6f). Moreover, Axin2 ISH showed a global increase in Wnt/β-Catenin signalling that extended to periportal hepatocytes at d2 post-PH (Supplementary Figure 7a, 7b), similar as seen in mice with RSPO1 injections.

The above findings indicate that LGR4/5 LOF impaired hepatocyte proliferation during liver regeneration as a consequence of abrogated Wnt signalling. It was recently shown that liver progenitor markers, including Lgr5, were upregulated d2 post-PH in periportal hepatocytes [34]. While RNA-Seq analysis confirmed upregulation of progenitor markers (Krt7, Tnfsrf12a) in control mice d2 post-PH when compared to naïve controls, Lgr5 expression was not increased (Supplementary Figure 7c). ISH analysis confirmed that Lgr5 was neither upregulated nor expressed in periportal hepatocytes of control mice at d2 post-PH. Similarly, Lgr4 ISH signals were not increased d2 post-PH (Supplementary Figure 7d-f). RNA-Seq of Lgr4/5dLKO compared to control livers at d2 post-PH further showed no change in liver progenitor marker expression (Sox9, Afp, Tnfsrf12a, Krt7, Krt19; Supplementary Figure 7g), suggesting that these cells did not contribute to impaired regeneration in Lgr4/5dLKO mice. RNA-Seq analysis further revealed that expression of Wnt target genes and genes regulating cell cycle progression and metabolism were reduced in Lgr4/5dLKO compared to control livers at d2 post-PH (Figure 6g). Likewise, gene sets implicated in cell cycle regulation and metabolism were downregulated in livers of regenerating Lgr4/5dLKO mice (Figure 6h). To study whether Lgr4/5LKO mice suffer from delayed liver regeneration, we additionally assessed hepatocyte proliferation during later stages of liver regeneration at d4 and d7 post-PH by Ki67 immunostaining (Figure 6i). Both at d4 and d7 hepatocyte proliferation was significantly increased in Lgr4/5LKO when compared to control mice (Figure 6j), similar to the delayed onset of proliferation seen in β-Catenin KO mice [14]. Despite increased proliferation at later phases of liver regeneration, Lgr4/5dLKO mice showed significant impairment in the magnitude and effectiveness of the regenerative response, resulting in a smaller final liver to body weight ratio compared to control mice (Figure 6k). This indicates that LGR4/5 are essential for the Wnt/β-Catenin-mediated early regenerative response which is required for establishing a normal liver to body weight ratio during regeneration, similar to our observations during liver development and homeostasis. Lineage tracing in Lgr5ki/R26-LacZ mice following PH indicated that pericentral LGR5+ hepatocytes do not extensively populate the liver during regrowth (Supplementary Figure 7h, 7i). Together, these findings highlight an important role for LGR4 and LGR5 in hepatocyte proliferation and liver size control during regeneration, with a dominant role for LGR4. Moreover, complete absence of Wnt/β-Catenin signalling in mice with LGR4/5 deletions established that the RSPO-LGR4/5-ZNRF3/RNF43 module is an essential mediator rather than a sole potentiator of Wnt/β-Catenin activity.

To study the role of RSPO in hepatic size control, we administered recombinant RSPO1 (10 mg/kg) or PBS twice weekly to Lgr4/5dLKO and control mice for 1 week, 2 weeks and 2 weeks followed by 4 weeks off-treatment (see scheme in Figure 5a). 1 week RSPO1 treatment in control mice significantly increased hepatocyte proliferation in all 3 liver zones when compared to PBS-injected control mice, with the strongest proliferative response in periportal hepatocytes. In Lgr4/5dLKO mice, RSPO1 did not increase hepatocyte proliferation (Figure 7a, 7b). Consequently, RSPO1 treatment in control mice resulted in increased liver weight when compared to PBS-injected mice, further increasing with prolonged treatment and decreasing upon RSPO1 withdrawal. In contrast, Lgr4/5dLKO mice did not gain liver weight following RSPO1 treatment (Figure 7c). Together, this indicates that RSPO1 increases liver size in a reversible and Lgr4/5-dependent manner. Likewise ZNRF3/RNF43 deletion in Znrf3/Rnf43dfl;R26CreERT2 mice resulted in a dramatic increase in hepatocyte proliferation 11 days post-TAM injections when compared to Znrf3/Rnf43dfl;R26CreERT2 mice without TAM (Figure 7d, 7e), showing a similar zonal profile as in RSPO1-injected mice. Increased proliferation of hepatocytes throughout the liver following ZNRF3/RNF43 deletions highlights the importance of these E3 ubiquitin ligases in restricting hepatocyte proliferation during liver homeostasis and suggests broad availability of Wnt receptors and ligands throughout the liver. Proliferation induced by RSPO1 injections or ZNRF3/RNF43 deletions was most evident in periportal hepatocytes, whereas Wnt/β-Catenin activity was higher in pericentral and parenchymal hepatocytes in RSPO1-injected mice. It is therefore possible that other pathways might cooperate with Wnt/β-Catenin to mediate this phenotype.

Finally, we assessed the potential of recombinant RSPO1 for improving liver regeneration. We therefore injected control mice with 10 mg/kg RSPO1 on 2 consecutive days, subjected the mice to PH and monitored liver regrowth by MRI (Figure 7f). While liver weight was not changed during the early phase (d2) of regeneration in either PBS- or RSPO1-injected mice, the latter showed a significant increase in liver weight at d7 post-PH (Figure 7g). Consistently, an MRI time-course showed increased liver size in RSPO1-injected mice during late phase regeneration (d6, d7) beyond levels of PBS-injected mice, whereas it was not changed before PH or at early stages of liver regeneration (Figure 7h, i). This indicates that increased RSPO1 levels overrule liver size control during regeneration. Most importantly, RSPO1 treatment accelerated liver regeneration since RSPO1-treated mice reached the final liver volume of control mice more rapidly. Together, RSPO-LGR4/5-ZNRF3/RNRF43 signalling acts as a hepatic growth/size rheostat during development, homeostasis and regeneration.

Discussion

Our data support a novel role for RSPO-LGR4/5-ZNRF3/RNF43 signalling in controlling spatiotemporal regulation of the hepatic Wnt/β-Catenin activity gradient and metabolic liver zonation. Impaired liver zonation in Lgr4/5dLKO mice is phenocopied in Znrf3ECD mice, whereas RSPO1 administration expanded the hepatic Wnt gradient in a reversible and LGR4/5-dependent manner. A recent study suggested that Wnt9b confers Wnt/β-Catenin activity restricted to the central vein [31]. We now found that RSPO1 injections or ZNRF3/RNF43 deletions expanded Wnt/β-Catenin activity to periportal hepatocytes, indicating that Wnt receptors and ligands are available throughout the liver. Moreover, Wnt9b deletion only reduced Wnt/β-Catenin activity [31] while LGR4/5 deletion resulted in complete loss of hepatic Wnt/β-Catenin signalling. This indicates that the RSPO-LGR4/5-ZNRF3/RNF43 module is not just potentiating Wnt activity but is essential for functional Wnt/β-Catenin signalling in the liver. While our data suggest that RSPO proteins confer local restriction of hepatic Wnt activity, their source and distribution remain to be identified.

The strongest increase in RSPO-induced proliferation around the portal vein was not paralleled by highest Wnt/β-Catenin activity in the region, indicating that other pathways might contribute to this phenotype. It was recently shown that YAP expression shows an inverse gradient to Wnt/β-Catenin activity in the liver [47]. Moreover, Wnt/β-Catenin activation promotes YAP signalling in other tissues [49]. It is possible that Wnt/β-Catenin-mediated YAP activation may contribute to periportal hepatocyte proliferation.

In a variety of tissue stem cell compartments, LGR4+ and LGR5+ cells are actively cycling and give rise to more mature cells with a high turnover [39-41]. Unlike other LGR5+ epithelial cells, pericentral LGR5+ hepatocytes did neither show overt proliferation nor gave rise to hepatocytes distant to the central vein, either under homeostasis conditions within an observation period of 18 months or during a 7-day post-PH liver regeneration period. Moreover, our EdU and Ki67 analyses in wild type mice could not detect increased proliferation of pericentral hepatocytes when compared to those of other liver zones. Our findings did not support the results of a recent study that was published during revision of our manuscript [31]. The authors proposed that pericentral hepatocytes comprise liver stem cells that repopulate large parts of the liver during homeostasis, whereas their potential during regeneration was not assessed[31]. Another recent study suggested that periportal hepatocytes with low SOX9 expression levels are liver stem cells with high regenerative capacity during homeostasis and drug-induced liver damage caused by zonal injury at the central vein [29]. It has been speculated that the site of injury determines the site of regeneration and that hepatocytes in different hepatic zones may mutually support liver regeneration in opposing sides [28]. Studying homeostatic hepatocyte renewal or regenerative response to PH, a paradigm model for liver regeneration that is not biased by zonal injury, we now show that LGR4+ hepatocytes throughout the liver contribute to liver homeostasis and regeneration. While the majority (>80%) of proliferating hepatocytes during homeostasis was found in the parenchyma, proliferation rates between the 3 zones were similar. During the peak regenerative response post-PH, pericentral hepatocytes proliferated less than parenchymal and periportal hepatocytes. Our findings are consistent with previous reports showing no zonal domination during liver homeostasis and reduced proliferation of pericentral hepatocytes following PH [42, 50]. This supports that parenchymal hepatocytes can have similar regenerative capacity as pericentral or periportal hepatocytes. Our data add to the emerging concept that there might not be just one liver stem cell compartment but that cells in different liver zones show increased regenerative potential depending on the injury [28, 32].

Despite recent advances in identifying cellular compartments that contribute to liver regeneration and maintenance [28-30, 32, 34, 44], the detailed mechanisms that confer spatiotemporal control of proliferation to maintain proper liver size remained elusive. We now show that increased RSPO-LGR4/5-ZNRF3/RNF43 signalling overrules the stop signals during liver regrowth or homeostasis, whereas LGR4/5 deletions result in hypoplastic livers. Likewise, LGR4/5 deletions impair liver regeneration, whereas RSPO1 injections accelerate regeneration. This supports the notion that the RSPO-LGR4/5-ZNRF3/RNF43 module acts as rheostat controlling liver growth and size. Our data further highlight important roles of ZNRF3 and RNF43 in restricting proliferation in the liver, consistent with *Rnf43* mutations observed in liver tumours [51].

Recently, periportal LGR5+ progenitor cells with bipotential progenitor characteristics were identified following CCl4 liver damage or diets that resulted in oval cell response in mice [33]. In contrast to our study, no LGR5+ cells were found in livers of naïve mice. It is possible that different genetic backgrounds between the mice used in our study (pure C57Bl/6) and those used in the above study (mixed C57Bl/6-Balb/c F1), different TAM dosing regimens or partial hepatic transgene silencing, as previously reported [33, 52], could explain these differences.

In contrast to LGR5, which was restricted to pericentral hepatocytes with high Wnt/β-Catenin pathway activity, LGR4 was broadly expressed in hepatocytes throughout the liver. Moreover, LGR5 has been described as a Wnt/β-Catenin target [39-41]. LGR5 deletion impaired pericentral hepatocyte proliferation post-PH, and combined deletion of LGR4 and LGR5 further impaired metabolic liver zonation than LGR4 deletion alone. This indicates that LGR5 is functionally relevant rather than just a marker of cells with high Wnt/β-Catenin activity. In contrast to LGR4 deletion, LGR5 deletion alone did not result in impaired Wnt/β-Catenin signalling. Loss of LGR5 expression as a consequence of LGR4 deletion further suggests a dominant role of LGR4 over LGR5, as previously shown in other tissues [26].

Our findings highlight novel roles for RSPO-LGR4/5-ZNRF3/RNF43 module in regulating Wnt/β-Catenin-mediated metabolic liver zonation and in acting as a growth/size control rheostat during liver development, homeostasis and regeneration. We further show that LGR4+ hepatocytes throughout the 3 liver zones contribute to homeostasis and regrowth. The growth-promoting effect of ectopic RSPO1 in livers highlights its potential use for regenerative therapies.

Materials and Methods

Immunostainings, ISH, RT-PCR and partial hepatectomy were essentially performed as described [53-55]. Detailed information on MRI, RNA-Seq, recombinant RSPO1 protein generation, mouse model design, image analysis and statistical analysis is available in the supplementary online material and methods. The raw RNA-sequencing reads are available in the NCBI Short Read Archive under the accession number SRP055521.

Acknowledgements

We thank Johann Wirsching, Carole Manneville, Marianne Lemaistre, Michel Haffner, Bettina Leonhard, Svenja Ley, Ning Guo, Tanya Lewis, Mei Li, Martin van de Velde, Daniel Breustedt, Hong Lei, Ryan Boomer, Stefan Zurbruegg, Ludovic Perrot, Francisco Cordoba, Sven Schuierer, Ana Arif and Julien Gfeller for technical assistance. For helpful discussion and critical reading of the manuscript we thank Elizabeth Wiellette, Gabi Hintzen, Bill Dietrich, Dong Liu, Frederic Bassilana, Christian Parker, Klaus Seuwen and Jeff Porter. This work was supported by the Leverhulme Trust ECF-2012-262 to Luke Boulter, SNF grant 310030B_147089 to Markus Heim, MRC Niche hub grant MR/K026666/1 to Stuart Forbes and the Novartis Institutes for BioMedical Research Program Office.

Conflict of interest statement. All authors except SF, LB, LMT, MHH, DC and MTD are employed by and/or shareholders of Novartis Pharma AG.

Figure legends

Figure 1. Lgr4 and Lgr5 are co-expressed in pericentral hepatocytes. a, GS and CYP2E1 co-staining in control mice. **b**, Venus expression in Tcf/Lef-Venus mice. **c**, Percent of hepatocytes expressing GS, CYP2E1 and Tcf/Lef-Venus in 3 cell layers around central and portal veins and in the parenchyma. n = 5 mice per group. **d**, **f**, **h**, Axin2 (**d**), Lgr4 and Lgr5 (**f**) and Znrf3 (**h**) ISH in control mice. **e**, **g**, **i**, Axin2 (**e**), Lgr4 and Lgr5 (**g**), and Znrf3 (**i**) ISH quantified in the indicated liver zones. n = (e) 5 mice where 4225 cells from 75

images were quantified, (g) 4 mice per group where 3380 cells from 60 images were quantified, and (i) 5 mice where 4341 cells from 75 images were quantified. **j**, LacZ staining in Rnf43-LacZ mice. **k**, Percent of hepatocytes expressing Rnf43-LacZ in the indicated liver zones. n = 4 mice. cv, central vein; pv, portal vein. Scale bars, (a, b) 100 µm, (magnification in a) 20 µm, (magnification in b) 50 µm, (d, f, h) 20 µm, (magnifications in d, f, h) 10 µm, (j) 100 µm and (magnifications in j) 50 µm.

Figure 2. Lgr4 and Lgr5 lineage tracing during liver homeostasis. **a**, **b**, LacZ staining in Lgr4ki/R26-LacZ mice showing LGR4+ hepatocytes after 10 days (**a**) or 10 months (**b**) of tracing. Arrowheads indicate clusters of LGR4+ hepatocytes. **c**, Clone size distribution of Lgr4ki/R26-LacZ+ hepatocytes. n = 3 mice. **d**, **e**, LacZ staining in Lgr5ki/R26-LacZ mice showing LGR5+ hepatocytes after 10 days (**d**) or 18 months (**e**) of tracing. Arrowheads (in b, e) indicate doublet cells. **f**, Clone size distribution of Lgr5ki/R26-LacZ+ hepatocytes. n = 4 mice. **g**, EGFP and HNF4α co-staining in Lgr4ki/R26-EGFP mice, showing EGFP+/HNF4α+ hepatocytes (arrowheads). **h**, tdTOM and GS co-staining in Lgr5ki/R26-tdTOM mice, showing tdTOM+/GS+ hepatocyte (arrowhead). **i**, Scheme depicting EdU injections in WT and Lgr5ki mice. **j**, EdU+ pericentral hepatocytes quantified in WT and Lgr5ki mice. n = 6 mice where 2195 (WT) and 1591 (Lgr5ki) cells were quantified. **k**, GS and EdU co-staining in control mice. Arrowheads point at EdU+ hepatocytes. **l**, EdU+ hepatocytes quantified in liver zones of control mice (percentage of EdU+ hepatocytes among total number of hepatocytes in respective zones). n = 6 mice where 2195 (CV), 3051 (PA) and 2555 (PV) cells from 90 images per zone were quantified. **m**, Distribution

of EdU+ hepatocytes in the indicated liver zones. n = 6 mice where 1296 cells were quantified. **n**, GS, biliary marker CK19 and Ki67 co-staining in control mice. Arrowheads point at Ki67+ hepatocytes. **o**, Ki67+ hepatocytes quantified in liver zones of control mice (percentage of Ki67+ hepatocytes among total number of hepatocytes in respective zones). **p**, Distribution of Ki67+ hepatocytes in the indicated liver zones. n = 4 mice where 891 cells from 60 images were quantified. cv, central vein; pv, portal vein. ns, not significant. Scale bars, (a, b, d, e) 50 µm and (g, h, k, n) 20 µm.

Figure 3. Lgr4 and Lgr5 receptors control liver zonation. **a**, Relative liver weight of the indicated mice. **b**, mRNA expression of different genes in the indicated mice. n = 5 mice per group. **c**, Lgr4 and Lgr5 ISH in the indicated mice. **d**, GS staining in the indicated mice. **e**, GS+ hepatocytes quantified in the indicated mice. **f**, CYP2E1 staining in the indicated mice. **g**, CYP2E1+ staining quantified in the indicated mice. **h**, Heatmap showing RNA expression of metabolic genes in livers of the indicated mice (yellow, high expression; blue, low expression). **i**, **j**, mRNA expression of pericentral (**i**) or periportal (**j**) metabolic genes in livers of the indicated mice. cv, central vein. n = 5 mice per group. *, $P<0.05$; **, $P<0.01$; ***, $P<0.001$; ****, $P<0.0001$; *****, $P<0.00001$. ns, not significant. Scale bars, (c) 20 µm, (d, f) 200 µm and (magnifications in d, f) 20 µm.

Figure 4. ZNRF3 and RNF43 control liver zonation. **a**, Scheme depicting Znrf3ECD/Axin2-LacZ mice that were given DOX or vehicle control on d1 and analysed on d7. **b, d, f**, LacZ (**b**), GS (**d**) or CYP2E1 (**f**) staining in Znrf3ECD/Axin2-LacZ mice +/- DOX. **c**, **e**, **g**, LacZ+ (**c**),

GS+ (**e**) or CYP2E1+ (**g**) staining quantified in Znrf3ECD/Axin2-LacZ mice +/- DOX. **h**, Scheme depicting Znrf3/Rnf43dfl;R26CreERT2 mice that were given TAM or vehicle control. **i**, **k**, GS (**i**) or CYP2E1 (**k**) staining in Znrf3/Rnf43dfl;R26CreERT2 mice +/- TAM. **j**, **l**, GS+ (**j**) or CYP2E1+ (**l**) staining quantified in Znrf3/Rnf43dfl;R26CreERT2 mice +/- TAM. cv, central vein; pv, portal vein. **, P<0.01; ***, P<0.001. Scale bars, (b) 100 µm, (magnifications in b) 50 µm, (d, f, i, k) 200 µm and (magnifications in d, f, i, k) 50 µm.

Figure 5. RSPO1 controls liver zonation via Lgr4 and Lgr5 receptors. **a**, Scheme depicting control, Lgr4/5dLKO and Tcf/Lef-Venus mice that were injected i.v. with RSPO1 or PBS for the indicated times. **b**, Axin2 ISH in control mice +/- RSPO1. **c**, Axin2 ISH quantified in control mice +/- RSPO1 in the indicated liver zones. n = 5 mice per group where 3392 cells (PBS) and 3774 cells (RSPO) from 75 images each were quantified. **d**, Venus expression in Tcf/Lef-Venus mice +/- RSPO1. **e**, Percent of Venus-expressing hepatocytes in Tcf/Lef-Venus mice +/- RSPO1 in the indicated liver zones. n = 4 mice (PBS) and 5 mice (RSPO). **f**, **h**, GS (**f**) and CYP2E1 (**h**) staining of control and Lgr4/5dLKO mice +/- RSPO1 for the indicated times. **g**, **i**, GS+ (**g**) or CYP2E1+ (**i**) staining quantified in control and Lgr4/5dLKO mice +/- RSPO1 for the indicated times. *, P<0.05; **, P<0.01; ***, P<0.001; ****, P<0.0001; ns, not significant. Scale bars, (b) 20 µm, (magnifications in b) 10 µm, (d) 100 µm, (magnifications in d) 50 µm and (f, h) 200 µm.

Figure 6. Loss of Lgr4 and Lgr5 results in impaired liver homeostasis and regeneration. **a**, Scheme depicting mice that were subjected to partial hepatectomy (PH) and analysed

at different time-points post-PH. **b**, Relative liver weight of the indicated mice at d2 post-PH. **c**, **d**, **e**, Ki67 staining and pericentral (**c**), parenchymal (**d**) and periportal (**e**) hepatocyte proliferation of the indicated mice at d2 post-PH. **f**, Axin2 mRNA expression in livers of the indicated mice. n = 5 mice (control + PH and Lgr4/5dLKO + PH), 6 mice (control - PH) and 7 mice (Lgr4/5dLKO - PH). **g**, Volcano plot showing genes differentially expressed in livers of the indicated mice. **h**, Gene sets downregulated in livers of the indicated mice. **i**, Ki67 staining in livers of the indicated mice at d4 and d7 post-PH. **j**, Liver cell proliferation quantified in the indicated mice at d4 and d7 post-PH. **k**, Relative liver weight of the indicated mice at d2, d4 and d7 post-PH. *, P<0.05; **, P<0.01; ***, P<0.001; ns, not significant. Scale bars, 100 µm.

Figure 7. RSPO1 promotes hepatocyte proliferation and liver regeneration via Lgr4 and Lgr5 receptors. **a**, Ki67 staining in livers of the indicated mice, showing Ki67+ hepatocytes (arrowheads). **b**, Hepatocyte proliferation quantified in liver zones of the indicated mice upon RSPO1 or PBS injection. **c**, Relative liver weight of the indicated mice. **d**, Ki67 staining in livers of the indicated mice, showing Ki67+ hepatocytes (arrowheads). **e**, Hepatocyte proliferation quantified in liver zones of the indicated mice. **f**, Scheme depicting control mice that were injected i.v. with RSPO1 or PBS on two consecutive days and subjected to PH. **g**, Relative liver weight of the indicated mice. **h**, Representative MRI liver sections of the indicated mice. **i**, Liver volume growth curve of the indicated mice following RSPO1 or PBS injection and PH. n = 6 male mice per group.

*, P<0.05; **, P<0.01; ***, P<0.001; ****, P<0.0001; ns, not significant. Scale bars, (a, d) 50 µm and (h) 6 mm.

References

1. Gebhardt, R. & Hovhannisyan, A. Organ patterning in the adult stage: the role of Wnt/beta-catenin signaling in liver zonation and beyond. *Developmental dynamics : an official publication of the American Association of Anatomists* **239**, 45-55 (2010).
2. Jungermann, K. & Katz, N. Functional specialization of different hepatocyte populations. *Physiological reviews* **69**, 708-764 (1989).
3. Jungermann, K. & Kietzmann, T. Zonation of parenchymal and nonparenchymal metabolism in liver. *Annual review of nutrition* **16**, 179-203 (1996).
4. Monga, S.P. Role and regulation of beta-catenin signaling during physiological liver growth. *Gene expression* **16**, 51-62 (2014).
5. Torre, C., Perret, C. & Colnot, S. Transcription dynamics in a physiological process: beta-catenin signaling directs liver metabolic zonation. *The international journal of biochemistry & cell biology* **43**, 271-278 (2011).
6. Michalopoulos, G.K. & DeFrances, M.C. Liver regeneration. *Science* **276**, 60-66 (1997).
7. Zaret, K.S. Regulatory phases of early liver development: paradigms of organogenesis. *Nature reviews. Genetics* **3**, 499-512 (2002).
8. Si-Tayeb, K., Lemaigre, F.P. & Duncan, S.A. Organogenesis and development of the liver. *Developmental cell* **18**, 175-189 (2010).
9. Burke, Z.D. *et al.* Liver zonation occurs through a beta-catenin-dependent, c-Myc-independent mechanism. *Gastroenterology* **136**, 2316-2324 e2311-2313 (2009).
10. Sekine, S., Lan, B.Y., Bedolli, M., Feng, S. & Hebrok, M. Liver-specific loss of beta-catenin blocks glutamine synthesis pathway activity and cytochrome p450 expression in mice. *Hepatology* **43**, 817-825 (2006).
11. Yang, J. *et al.* beta-catenin signaling in murine liver zonation and regeneration: a Wnt-Wnt situation! *Hepatology* **60**, 964-976 (2014).
12. Niehrs, C. The complex world of WNT receptor signalling. *Nature reviews. Molecular cell biology* **13**, 767-779 (2012).
13. Benhamouche, S. *et al.* Apc tumor suppressor gene is the "zonation-keeper" of mouse liver. *Developmental cell* **10**, 759-770 (2006).
14. Apte, U. *et al.* Beta-catenin activation promotes liver regeneration after acetaminophen-induced injury. *The American journal of pathology* **175**, 1056-1065 (2009).
15. Boulter, L. *et al.* Macrophage-derived Wnt opposes Notch signaling to specify hepatic progenitor cell fate in chronic liver disease. *Nature medicine* **18**, 572-579 (2012).

16. Monga, S.P., Pediaditakis, P., Mule, K., Stolz, D.B. & Michalopoulos, G.K. Changes in WNT/beta-catenin pathway during regulated growth in rat liver regeneration. *Hepatology* **33**, 1098-1109 (2001).
17. Nejak-Bowen, K. & Monga, S.P. Wnt/beta-catenin signaling in hepatic organogenesis. *Organogenesis* **4**, 92-99 (2008).
18. Nejak-Bowen, K.N. *et al.* Accelerated liver regeneration and hepatocarcinogenesis in mice overexpressing serine-45 mutant beta-catenin. *Hepatology* **51**, 1603-1613 (2010).
19. Sekine, S., Gutierrez, P.J., Lan, B.Y., Feng, S. & Hebrok, M. Liver-specific loss of beta-catenin results in delayed hepatocyte proliferation after partial hepatectomy. *Hepatology* **45**, 361-368 (2007).
20. Carmon, K.S., Gong, X., Lin, Q., Thomas, A. & Liu, Q. R-spondins function as ligands of the orphan receptors LGR4 and LGR5 to regulate Wnt/beta-catenin signaling. *Proceedings of the National Academy of Sciences of the United States of America* **108**, 11452-11457 (2011).
21. de Lau, W. *et al.* Lgr5 homologues associate with Wnt receptors and mediate R-spondin signalling. *Nature* **476**, 293-297 (2011).
22. Glinka, A. *et al.* LGR4 and LGR5 are R-spondin receptors mediating Wnt/beta-catenin and Wnt/PCP signalling. *EMBO reports* **12**, 1055-1061 (2011).
23. Ruffner, H. *et al.* R-Spondin potentiates Wnt/beta-catenin signaling through orphan receptors LGR4 and LGR5. *PloS one* **7**, e40976 (2012).
24. Hao, H.X. *et al.* ZNRF3 promotes Wnt receptor turnover in an R-spondin-sensitive manner. *Nature* **485**, 195-200 (2012).
25. Koo, B.K. *et al.* Tumour suppressor RNF43 is a stem-cell E3 ligase that induces endocytosis of Wnt receptors. *Nature* **488**, 665-669 (2012).
26. Kinzel, B. *et al.* Functional roles of Lgr4 and Lgr5 in embryonic gut, kidney and skin development in mice. *Developmental biology* **390**, 181-190 (2014).
27. Koo, B.K. & Clevers, H. Stem cells marked by the R-spondin receptor LGR5. *Gastroenterology* **147**, 289-302 (2014).
28. Bird, T.G. & Forbes, S.J. Two Fresh Streams to Fill the Liver's Hepatocyte Pool. *Cell stem cell* **17**, 377-378 (2015).
29. Font-Burgada, J. *et al.* Hybrid Periportal Hepatocytes Regenerate the Injured Liver without Giving Rise to Cancer. *Cell* **162**, 766-779 (2015).
30. Lu, W.Y. *et al.* Hepatic progenitor cells of biliary origin with liver repopulation capacity. *Nature cell biology* **17**, 971-983 (2015).
31. Wang, B., Zhao, L., Fish, M., Logan, C.Y. & Nusse, R. Self-renewing diploid Axin2(+) cells fuel homeostatic renewal of the liver. *Nature* **524**, 180-185 (2015).
32. Zaret, K.S. Regenerative biology: Maintaining liver mass. *Nature* **524**, 165-166 (2015).
33. Huch, M. *et al.* In vitro expansion of single Lgr5+ liver stem cells induced by Wnt-driven regeneration. *Nature* **494**, 247-250 (2013).
34. Karaca, G. *et al.* TWEAK/Fn14 signaling is required for liver regeneration after partial hepatectomy in mice. *PloS one* **9**, e83987 (2014).
35. Colnot S., P.C. Liver Zonation, in *Molecular Pathology of Liver Diseases* Vol. Molecular Pathology Library 5. (ed. S.P. Monga) (Springer Science and Business Media, 2011).

36. Ferrer-Vaquer, A. *et al.* A sensitive and bright single-cell resolution live imaging reporter of Wnt/ss-catenin signaling in the mouse. *BMC developmental biology* **10**, 121 (2010).
37. Gerbal-Chaloin, S. *et al.* The WNT/beta-catenin pathway is a transcriptional regulator of CYP2E1, CYP1A2, and aryl hydrocarbon receptor gene expression in primary human hepatocytes. *Molecular pharmacology* **86**, 624-634 (2014).
38. Soriano, P. Generalized lacZ expression with the ROSA26 Cre reporter strain. *Nature genetics* **21**, 70-71 (1999).
39. Barker, N. *et al.* Identification of stem cells in small intestine and colon by marker gene Lgr5. *Nature* **449**, 1003-1007 (2007).
40. Clevers, H., Loh, K.M. & Nusse, R. Stem cell signaling. An integral program for tissue renewal and regeneration: Wnt signaling and stem cell control. *Science* **346**, 1248012 (2014).
41. Snippert, H.J. *et al.* Lgr6 marks stem cells in the hair follicle that generate all cell lineages of the skin. *Science* **327**, 1385-1389 (2010).
42. Klochendler, A. *et al.* A transgenic mouse marking live replicating cells reveals in vivo transcriptional program of proliferation. *Developmental cell* **23**, 681-690 (2012).
43. Burkhardt, S., Bahnemann, R., Failing, K. & Reinacher, M. Zonal distribution of cell proliferation in the liver of untreated B6C3F1 and C57BL mice. *Toxicologic pathology* **32**, 100-105 (2004).
44. Miyajima, A., Tanaka, M. & Itoh, T. Stem/progenitor cells in liver development, homeostasis, regeneration, and reprogramming. *Cell stem cell* **14**, 561-574 (2014).
45. Gougelet, A. *et al.* T-cell factor 4 and beta-catenin chromatin occupancies pattern zonal liver metabolism in mice. *Hepatology* **59**, 2344-2357 (2014).
46. Clevers, H. Wnt/beta-catenin signaling in development and disease. *Cell* **127**, 469-480 (2006).
47. Fitamant, J. *et al.* YAP Inhibition Restores Hepatocyte Differentiation in Advanced HCC, Leading to Tumor Regression. *Cell reports* (2015).
48. Marti, P. *et al.* YAP promotes proliferation, chemoresistance, and angiogenesis in human cholangiocarcinoma through TEAD transcription factors. *Hepatology* (2015).
49. Azzolin, L. *et al.* YAP/TAZ incorporation in the beta-catenin destruction complex orchestrates the Wnt response. *Cell* **158**, 157-170 (2014).
50. Bralet, M.P., Branchereau, S., Brechot, C. & Ferry, N. Cell lineage study in the liver using retroviral mediated gene transfer. Evidence against the streaming of hepatocytes in normal liver. *The American journal of pathology* **144**, 896-905 (1994).
51. Ong, C.K. *et al.* Exome sequencing of liver fluke-associated cholangiocarcinoma. *Nature genetics* **44**, 690-693 (2012).
52. Tchorz, J.S. *et al.* A modified RMCE-compatible Rosa26 locus for the expression of transgenes from exogenous promoters. *PloS one* **7**, e30011 (2012).
53. Dill, M.T. *et al.* Constitutive Notch2 signaling induces hepatic tumors in mice. *Hepatology* **57**, 1607-1619 (2013).
54. Mitchell, C. & Willenbring, H. A reproducible and well-tolerated method for 2/3 partial hepatectomy in mice. *Nature protocols* **3**, 1167-1170 (2008).

55. Wieland, S. *et al.* Simultaneous detection of hepatitis C virus and interferon stimulated gene expression in infected human liver. *Hepatology* **59**, 2121-2130 (2014).

Figure 1
Planas-Paz & Orsini et al.

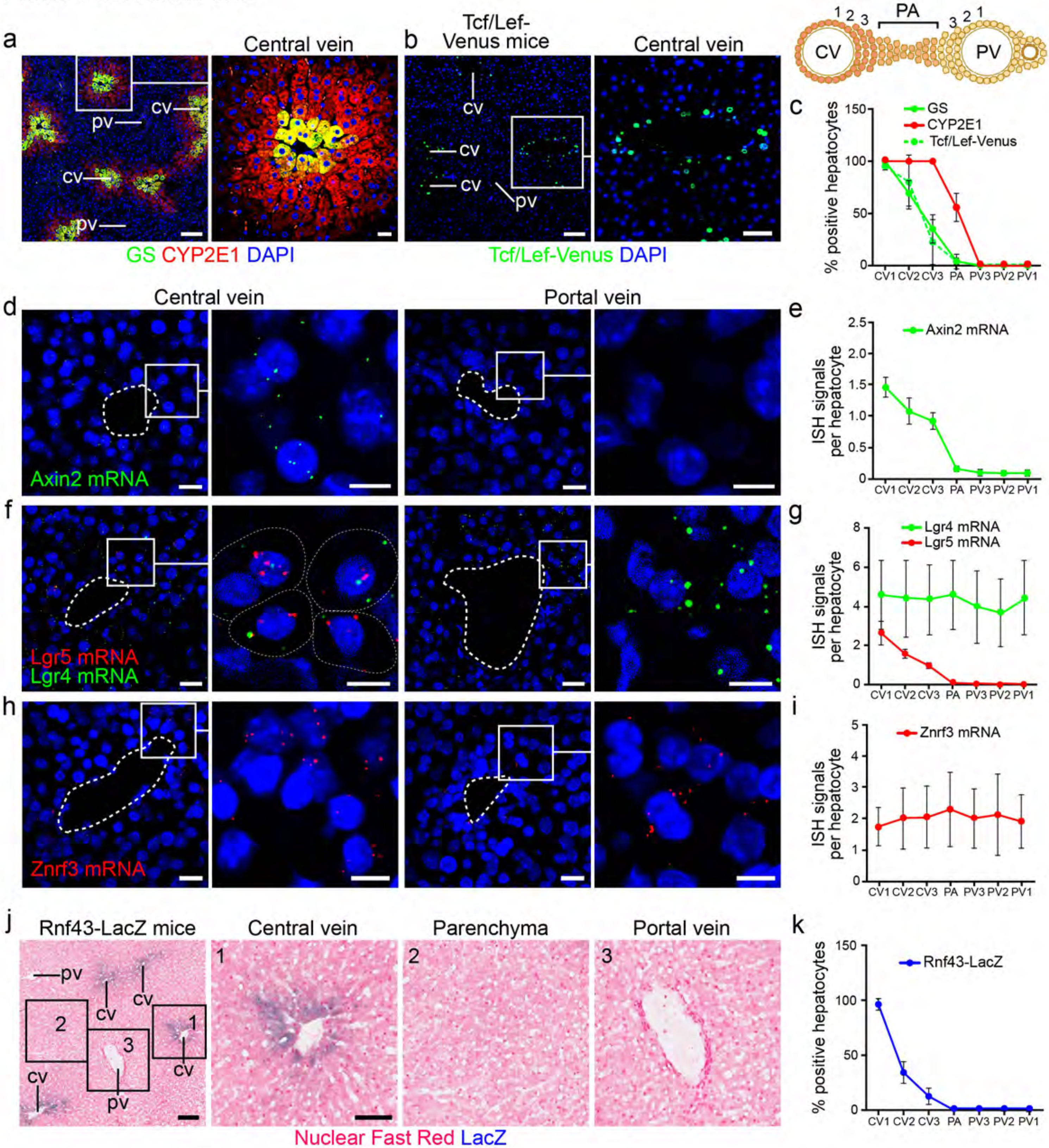

Figure 2

Planas-Paz & Orsini et al.

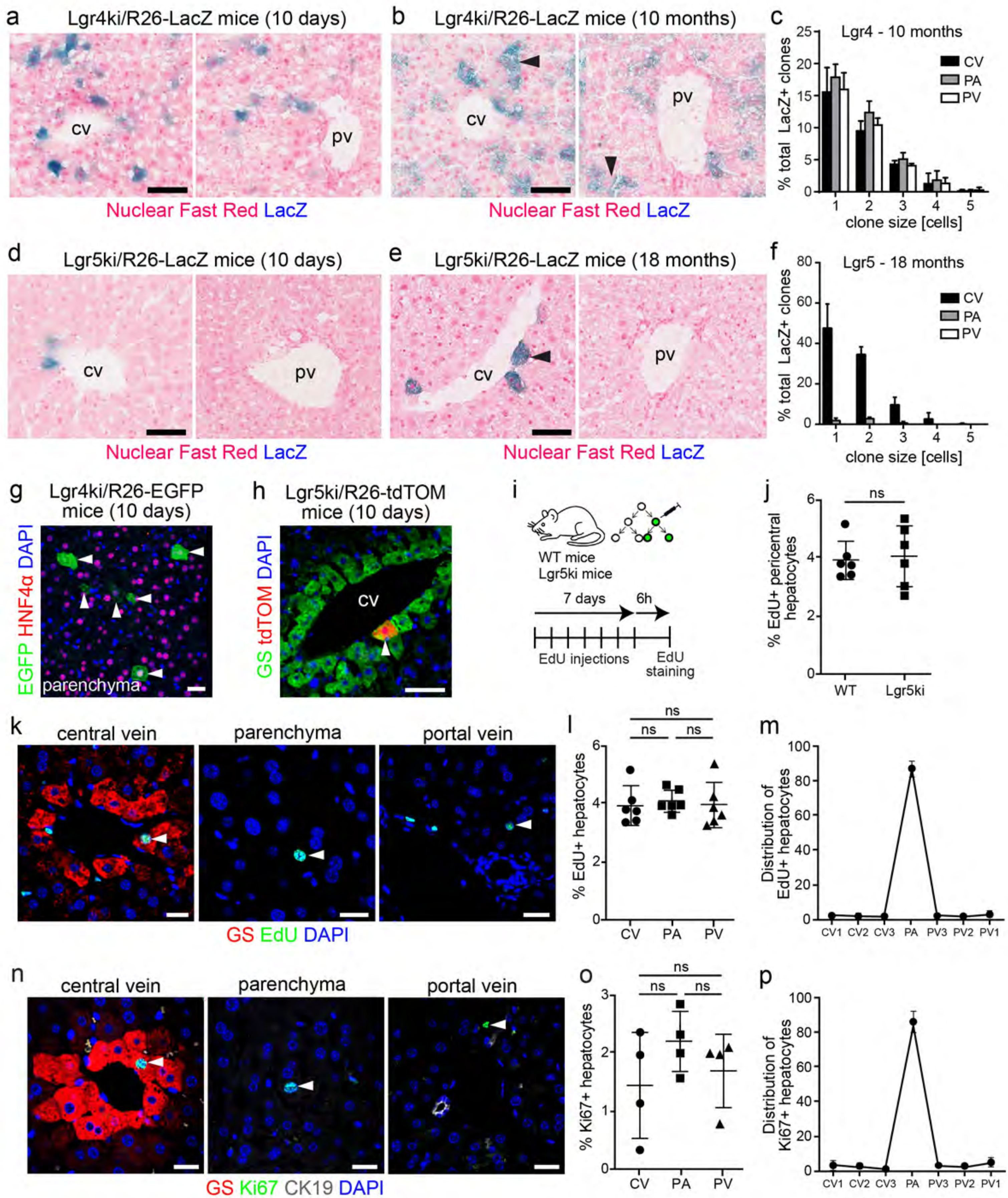

Figure 3

Planas-Paz & Orsini et al.

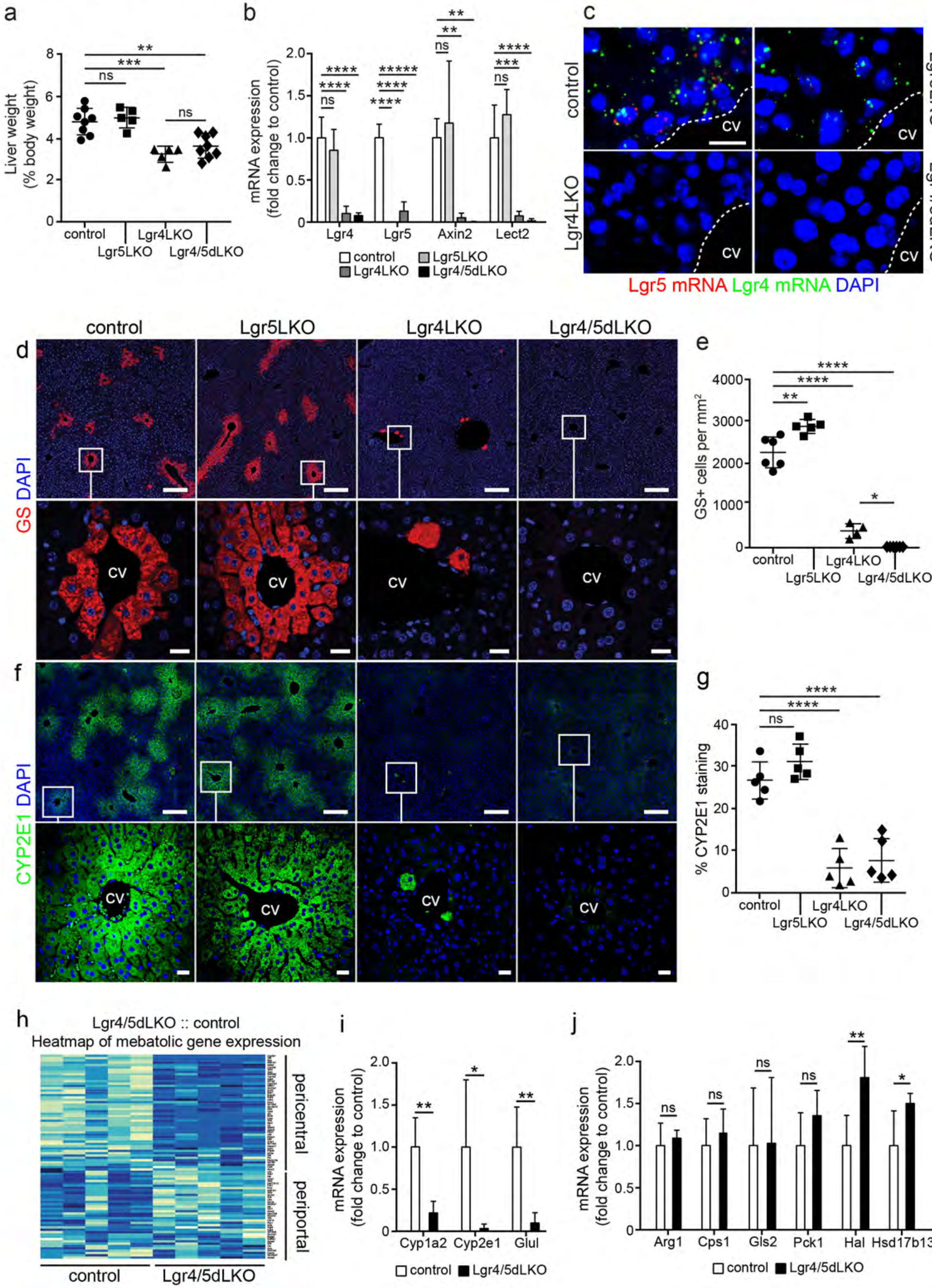

Figure 4

Planas-Paz & Orsini et al.

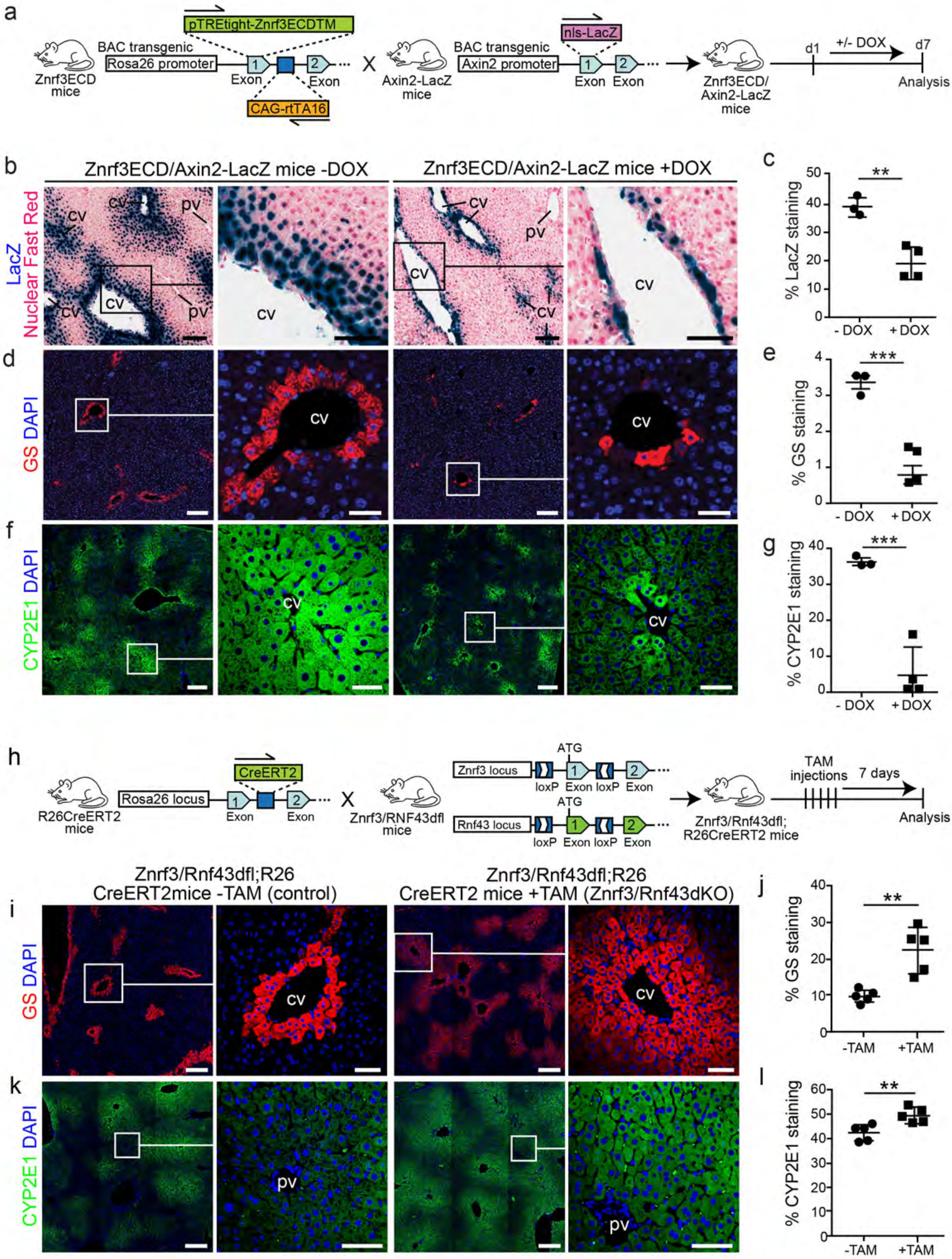

Figure 5

Planas-Paz & Orsini et al.

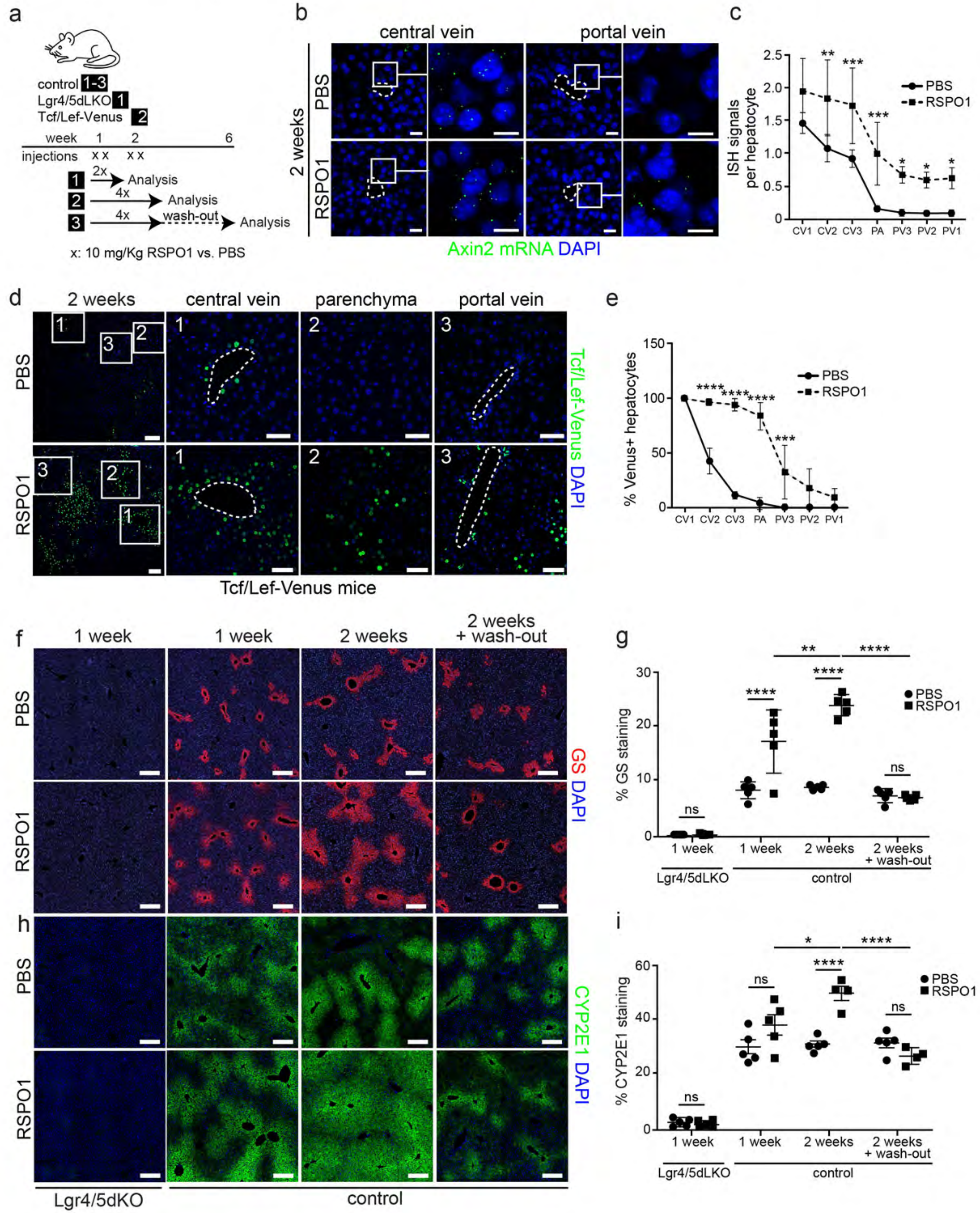

Figure 6

Planas-Paz & Orsini et al.

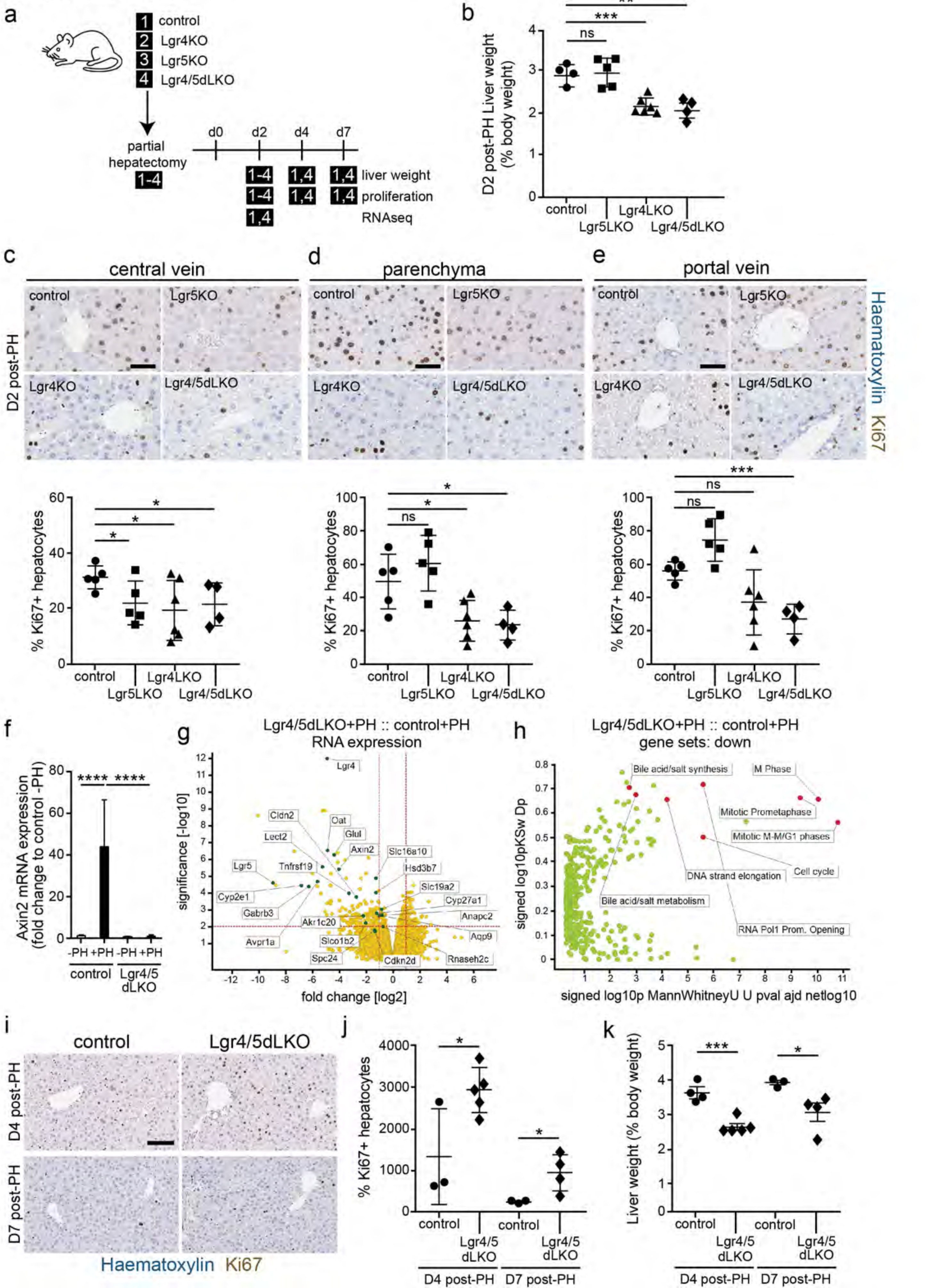

Figure 7

Planas-Paz & Orsini et al.

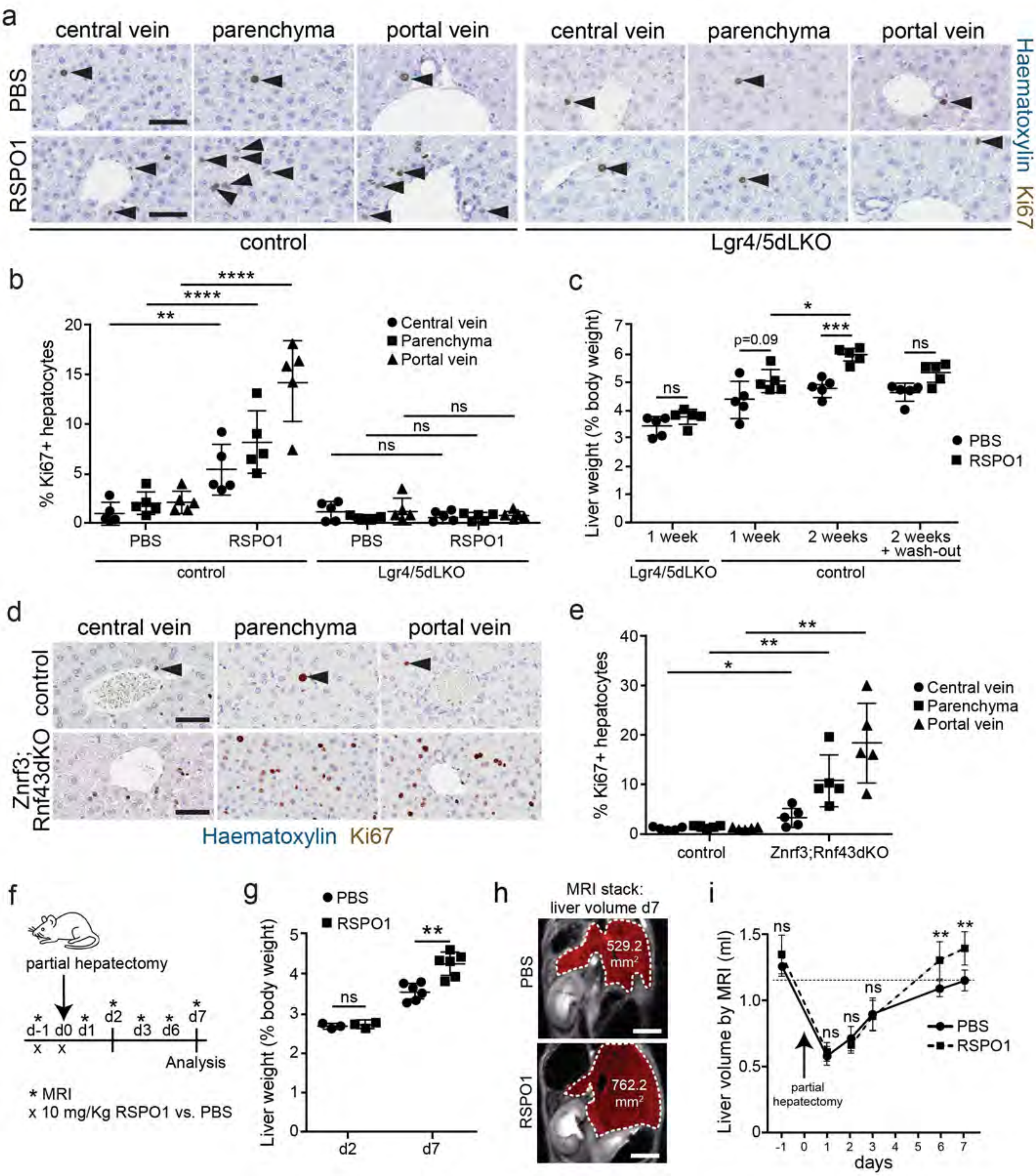

Supplementary Figure 1

Planas-Paz & Orsini et al.

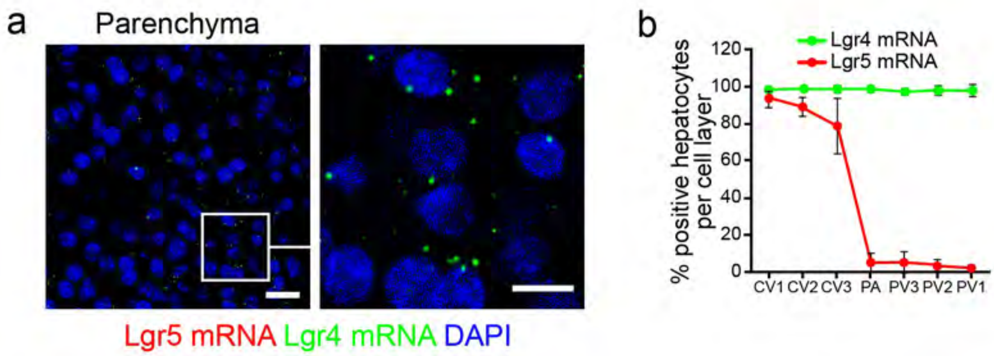

Supplementary Figure 2

Planas-Paz & Orsini et al.

a

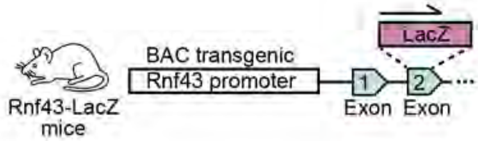

b

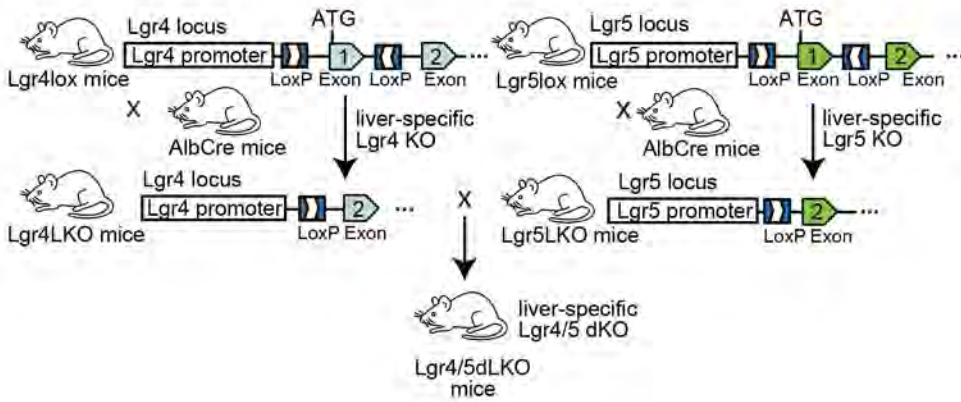

Supplementary Figure 3

Planas-Paz & Orsini et al.

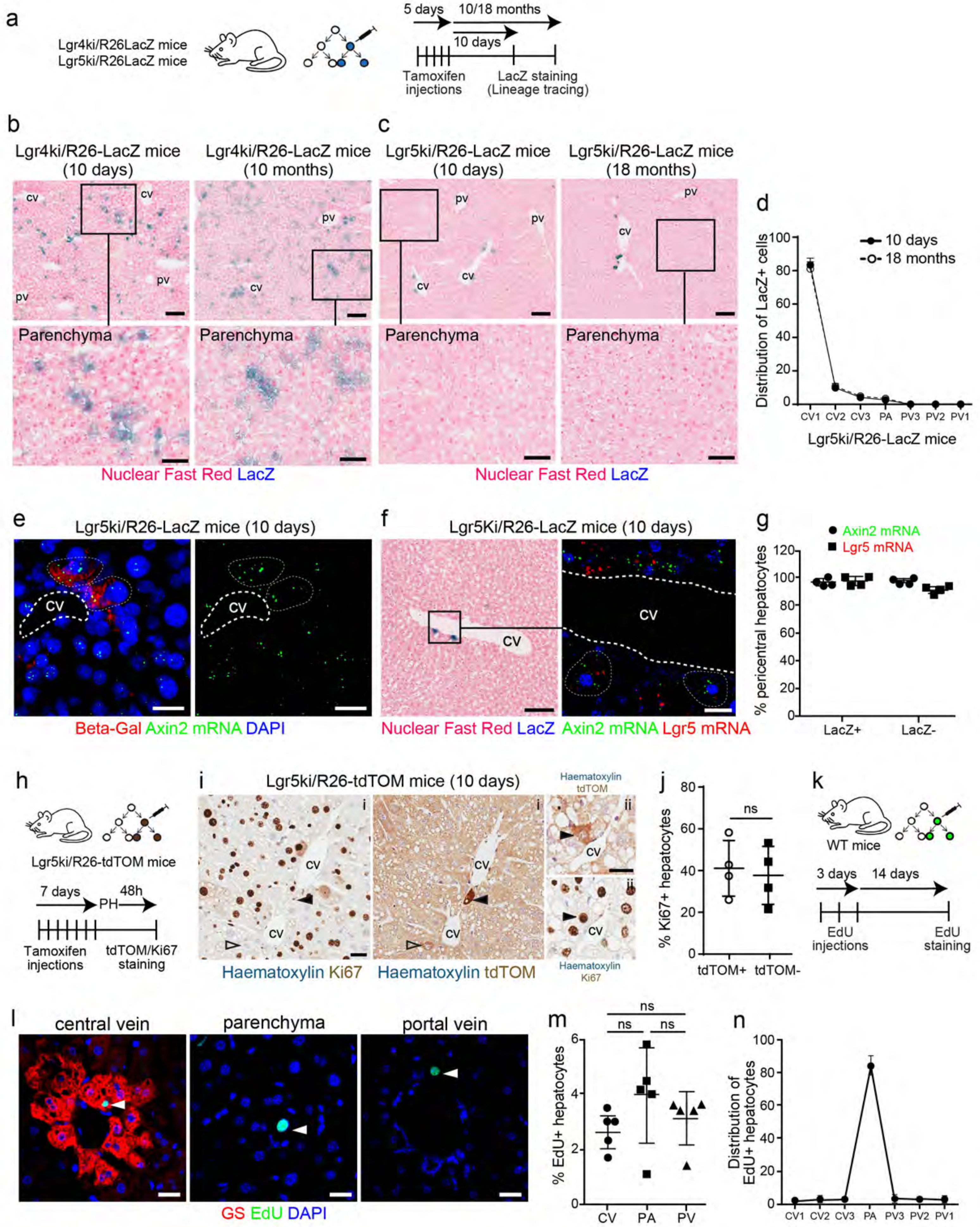

Supplementary Figure 4

Planas-Paz & Orsini et al.

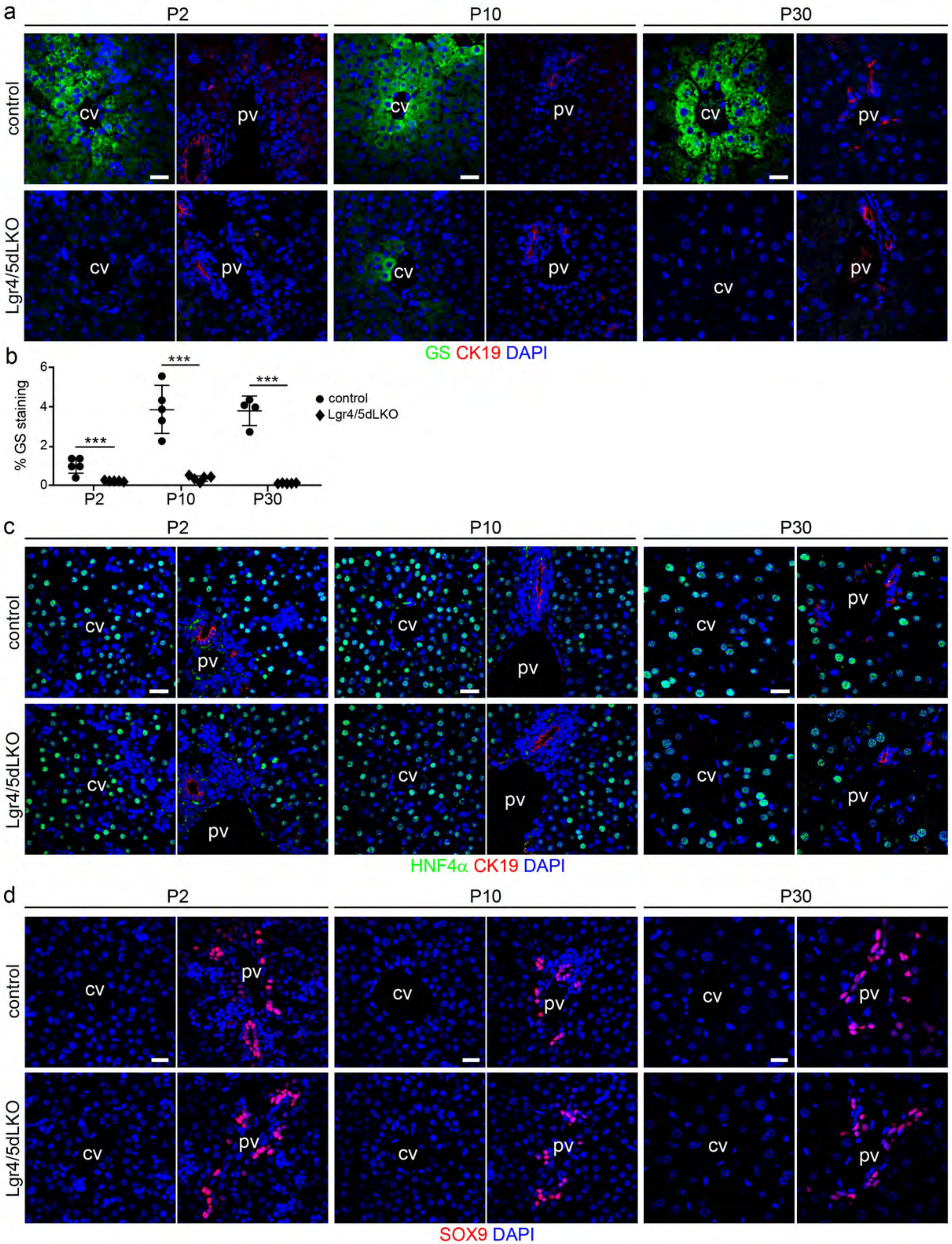

Supplementary Figure 5

Planas-Paz & Orsini et al.

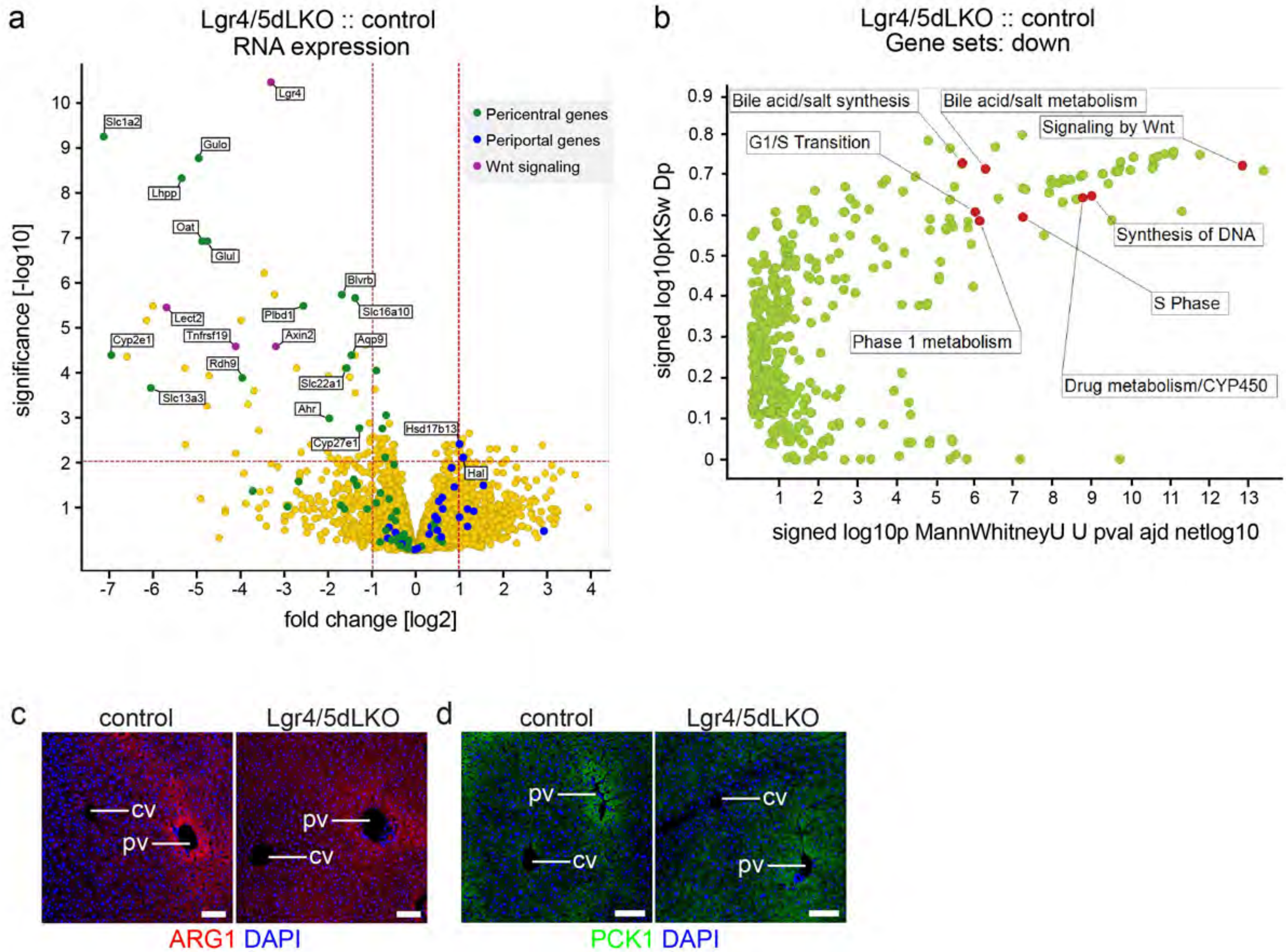

Supplementary Figure 6

Planas-Paz & Orsini et al.

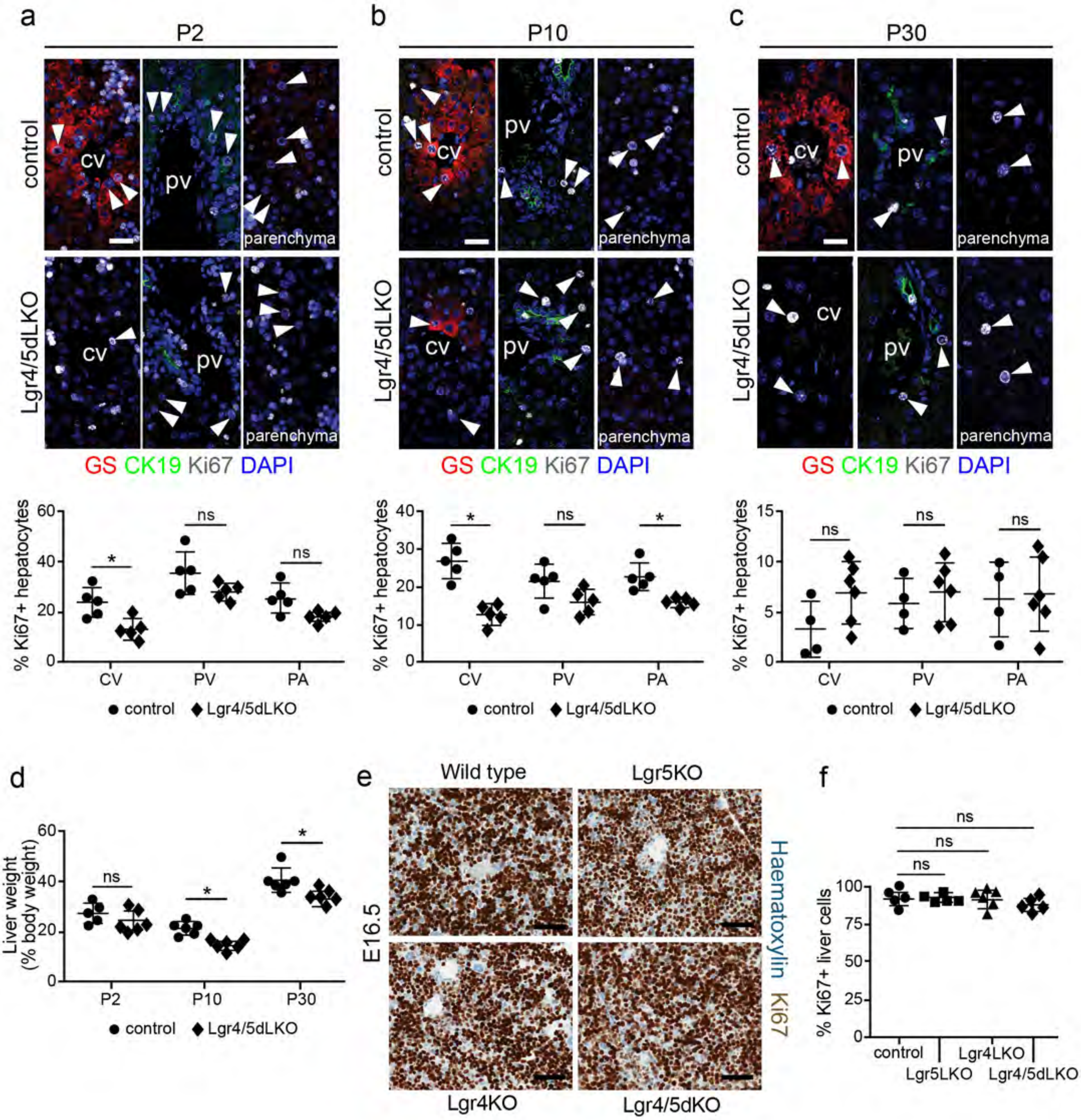

Supplementary Figure 7

Planas-Paz & Orsini et al.